

Slope failure and mass transport processes along the Queen Charlotte Fault Zone, western British Columbia




H. GARY GREENE^{1*}, J. VAUGHN BARRIE², DANIEL S. BROTHERS³,
JAMES E. CONRAD³, KIM CONWAY², AMY E. EAST³, RANDY ENKIN²,
KATHERINE L. MAIER², STUART P. NISHENKO⁴,
MAUREEN A. L. WALTON³ & KRISTIN M. M. ROHR²

¹*Moss Landing Marine Laboratories and Tomolo Mapping Laboratory,
142 Anchor Rock Lane, Eastsound, WA 98245, USA*

²*Geological Survey of Canada (Pacific), 9860 West Saanich Road, Sidney,
BC V8L 4B2, Canada*

³*US Geological Survey, Pacific Coastal and Marine Center, 2885 Mission Street,
Santa Cruz, CA 95060, USA*

⁴*Pacific Gas & Electric Company, 77 Beale Street, San Francisco,
CA 94105, USA*

 J.E.C., 0000-0001-6655-694X; K.L.M., 0000-0003-2908-3340;
M.A.L.W., 0000-0001-8496-463X; K.M.M.R., 0000-0001-6347-712X

*Correspondence: greeneg@mlml.calstate.edu

Abstract: Multibeam echosounder (MBES) images, 3.5 kHz seismic-reflection profiles and piston cores obtained along the southern Queen Charlotte Fault Zone are used to map and date mass-wasting events at this transform margin – a seismically active boundary that separates the Pacific Plate from the North American Plate. Whereas the upper continental slope adjacent to and east (upslope) of the fault zone offshore of the Haida Gwaii is heavily gullied, few large-sized submarine landslides in this area are observed in the MBES images. However, smaller submarine seafloor slides exist locally in areas where fluid flow appears to be occurring and large seafloor slides have recently been detected at the base of the steep continental slope just above its contact with the abyssal plain on the Queen Charlotte Terrace. In addition, along the subtle slope re-entrant area offshore of the Dixon Entrance shelf bathymetric data suggest that extensive mass wasting has occurred in the vicinity of an active mud volcano venting gas. We surmise that the relative lack of submarine slides along the upper slope in close proximity to the Queen Charlotte Fault Zone may be the result of seismic strengthening (compaction and cohesion) of a sediment-starved shelf and slope through multiple seismic events.

The Queen Charlotte–Fairweather (QC–FW) Fault System is a major structural feature that extends from north of Vancouver Island, Canada to well into the bight of the Gulf of Alaska (Fig. 1). This system represents a major transform boundary that separates the Pacific Plate from the North American Plate, similar to the San Andreas (SAF) Fault System of California (Atwater 1970; Plafker *et al.* 1978). The length of the QC–FW fault system is 1330 km, slightly longer than the SAF, with an estimated width of 1–5 km and approximately 75% of the length located offshore (Carlson *et al.* 1985). Recently, most of the fault zone through SE Alaska has been imaged in detail using multibeam echosounder (MBES) data and other geophysical

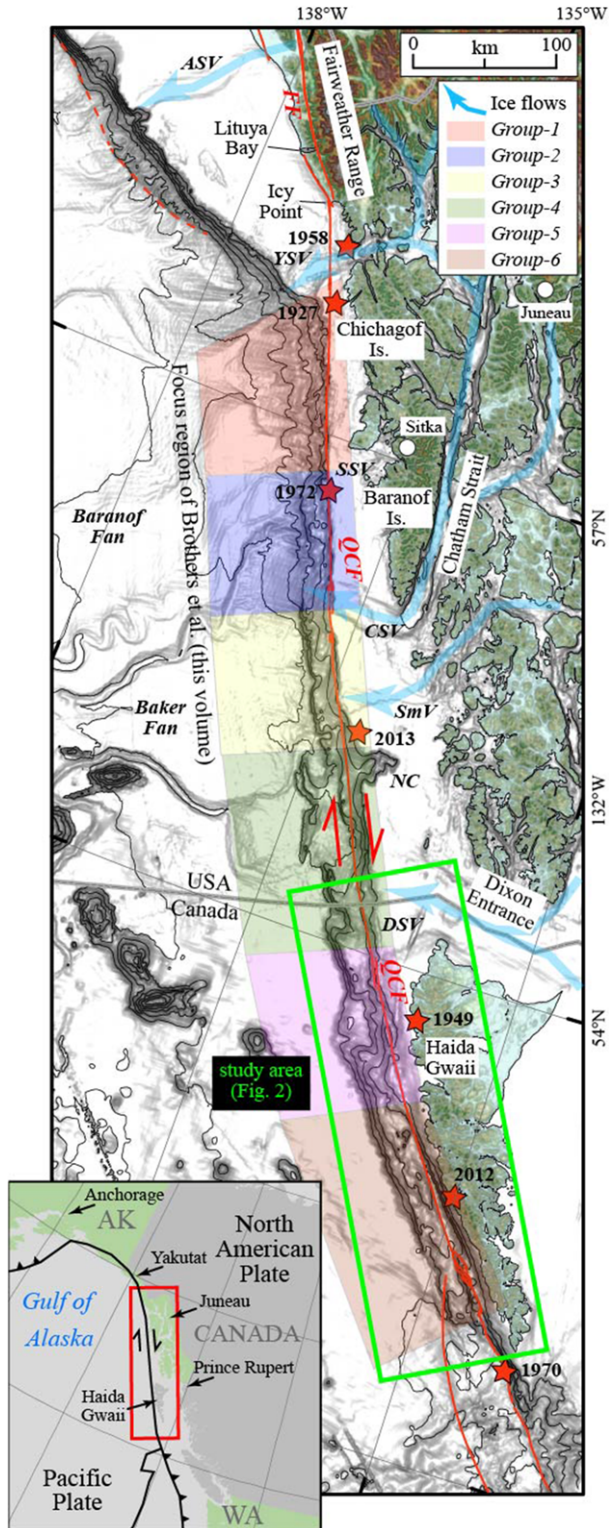
techniques (Brothers *et al.* 2017, this volume, in press).

In the south, the Queen Charlotte (QC) Fault System extends for over 350 km along the western margin of British Columbia and offshore of the Haida Gwaii (formerly Queen Charlotte Islands) archipelago (Fig. 1). It is a near-vertical fault zone that is seismically active down to approximately 21 km (Hyndman & Ellis 1981) with a mainly right-lateral transform motion of approximately 50–60 mm a⁻¹ (Prims *et al.* 1997; Rohr *et al.* 2000). Barrie *et al.* (2013) presented MBES data along the QC Fault Zone offshore of southern and central Haida Gwaii, which assisted with documenting the fault morphology and identifying features associated with

From: LINTERN, D. G., MOSHER, D. C., MOSCARDELLI, L. G., BOBROWSKY, P. T., CAMPBELL, C., CHAYTOR, J. D., CLAGUE, J. J., GEORGIOPOULOU, A., LAJEUNESSE, P., NORMANDEAU, A., PIPER, D. J. W., SCHERWATH, M., STACEY, C. & TURMEL, D. (eds) *Subaqueous Mass Movements*. Geological Society, London, Special Publications, **477**, <https://doi.org/10.1144/SP477.31>

© 2018 The Author(s). Published by The Geological Society of London. All rights reserved.

For permissions: <http://www.geolsoc.org.uk/permissions>. Publishing disclaimer: www.geolsoc.org.uk/pub_ethics



MASS TRANSPORT ALONG QUEEN CHARLOTTE FAULT ZONE

localized deformation along the fault (e.g. step-overs, submarine canyons, gullies and a submarine slide adjacent to the fault). This paper presents the first detailed examination of mass-transport processes evident along the QC Fault Zone south of the USA (Alaska)–Canada International Boundary (Figs 1 & 2). In this companion paper to Brothers *et al.* (this volume, in press), which describes mass-transport processes associated with the QC Fault Zone in Alaska to the north of our study area, we examine the geomorphic and sedimentary processes that dominate the southern QC Fault Zone using new sediment cores and multibeam bathymetric data.

Background

Unlike the QC Fault Zone, much is known of the SAF and other transform fault systems throughout the world, primarily because a considerable number of these systems are located on land and easily accessible. Since the QC transform is primarily located offshore, shipboard and remotely collected data are required to study the fault system. Until recently, moderate- to large-magnitude earthquakes, of which there have been many (see Fig. 1), have been used to locate the QC Fault and understand its motion. The 1949 surface-wave magnitude M_s 8.1 (a moment magnitude of M_w 7.9) Queen Charlotte Islands (Haida Gwaii) earthquake is the largest historical earthquake to have occurred in Canada (Fig. 1). This strike-slip event had an estimated rupture length of between 265 and 490 km (up to 300 km north and 190 km south of the epicentre) and an average co-seismic displacement of 4.0–7.5 m (Rogers 1983; Bostwick 1984; Lay *et al.* 2013). The 2013 M_w 7.5 Craig strike-slip earthquake occurred near the northern end of the 1949 rupture zone (e.g. Ding *et al.* 2015; Tréhu *et al.* 2015).

In contrast to the predominately strike-slip motion along the central and northern portions of the QC Fault Zone, plate motion along the southern portion is strike-slip but expresses some obliquity (e.g. Hyndman & Hamilton 1993; Brothers *et al.*

2017). The 2012 Haida Gwaii (M_w 7.8) earthquake involved slightly oblique thrust faulting on a shallow-dipping fault plane whose strike is sub-parallel to the QC Fault Zone (e.g. Lay *et al.* 2013).

In addition, several other recent large earthquakes have been reported along the fault zone (Page 1969; Carlson *et al.* 1985; Lisowski *et al.* 1987). This seismicity includes a shallow (<1 km deep) moderate-magnitude earthquake (M_L 5.7 on 6 January 2000) along the QC–FW Fault Zone offshore of Yakutat and NW of the entrance to Cross Sound (see the Alaska Earthquake Information Center website), a deeper (10 km) moderate-magnitude (M_L 5.9) earthquake that occurred in the south on 17 February 2001 and the 2004 Chatham Strait (M_L 6.8) Fault Zone on 28 June 2004. The latest earthquake occurred on 16 January 2017, a magnitude 4.3 event located on the QC Fault offshore of Elfin Cove (offshore of Cross Sound), approximately 145 km north of Sitka. Based on stress distribution, a continued rise in earthquake hazard for the QC Fault Zone is anticipated (Bufe 2005).

A geomorphological comparison of the continental margin associated with the entire QC Fault Zone has recently been undertaken for the first time. Brothers *et al.* (this volume, in press) present a classification of the first-order, across-margin shape of the continental shelf, slope and rise that they use to examine potential relationships between form and process dominance. The authors split the margin into six morphological groupings (see Fig. 1), which record a gradational change from north to south. The northernmost and southernmost groups are defined by two basic end members. The northernmost grouping (groups 1–3) is characterized by concave slope profiles, gentle slopes (<6°) and relatively low along-strike variation – features characteristic of sediment-dominated margins. Transpression increases southwards along the QC Fault Zone with the slope physiography dominated by deformational structures and very steep seafloor profiles (>30°) that lead to sediment bypass. The southernmost grouping (west of Haida Gwaii) defines the tectonically dominated groups 4–6 of Brothers *et al.*

Fig. 1. Topography (colour) and bathymetry (black & white) of NW British Columbia, Canada and SE Alaska showing the location and trend of the Queen Charlotte–Fairweather Fault System and other faults (red lines). The green box outlines the area of study (Fig. 2). The grey line shows approximate location of the USA–Canadian border. Red stars and dates mark approximate locations of major earthquake epicentres. Coloured boxes represent the continental margin geomorphic groups constructed from bathymetric profiles across the shelf, slope and abyss (from Brothers *et al.* this volume, in press). Blue lines and arrows illustrate the direction and route of glacial advances during the LGM; however, recent studies by Lyles *et al.* (2017) indicate that the ice flow was north and not west at Dixon Entrance, CSV, Chatham Sea Valley; DSV, Dixon Sea Valley; NC, Noyes Canyon; SSV, Sitka Sea Valley; SmV, Sumner Sea Valley; YSV, Yakobi Sea Valley; Source: NOAA and Coastal Relief Model. Modified after Brothers *et al.* (this volume, in press). Shaded-relief bathymetry data (grey) shown here and in Fig. 2 and 3d from ETOPO1 data (National Geophysical Data Center 2013), and a United Nations Commission Law of the Sea (UNCLOS) dataset (Center for Coastal and Ocean Mapping Joint Hydrographic Center 2010).

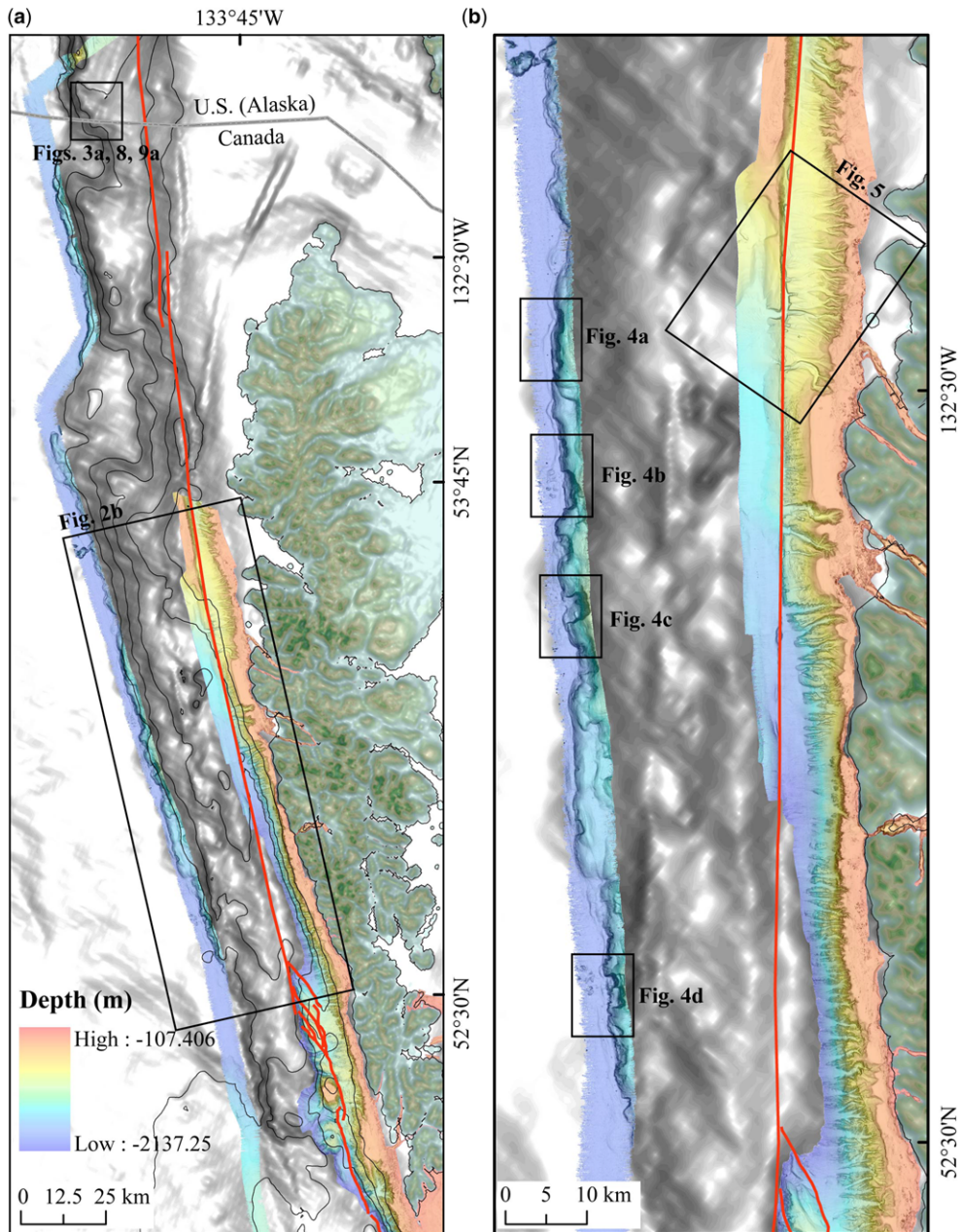


Fig. 2. Area of investigation offshore of western British Columbia, Canada: (a) map showing the location of the two multibeam echosounder bathymetric datasets used in this study (blue, *Sikuliaq* bathymetry; multicoloured, Canadian Hydrographic Services data; red line, QC Fault Zone; the white area at the top is Dixon Entrance; black-lined boxes show the locations of figures); and (b) expanded view offshore of the central Haida Gwaii showing locations of figures (black-outlined boxes).

(this volume, in press), which are characterized by elongate ridgelines, very steep slopes ($>30^\circ$) and sediment bypass to the continental rise.

Our area of study includes the continental margin geomorphic groups 4–6 that are described by Brothers *et al.* (this volume, in press, their figs 1 & 2) and

MASS TRANSPORT ALONG QUEEN CHARLOTTE FAULT ZONE

which we summarize here. Group 4 extends from Noyes Canyon to the northern tip of Haida Gwaii, which includes the Dixon Entrance Sea Valley (Fig. 1). We consider Dixon Entrance to be one of the major sediment routing pathways during the Quaternary, although Lyles *et al.* (2017) and James Baichtal (pers. comm. 2017) present evidence that the major ice streams during the Last Glacial Maximum (LGM) were north of Dixon Entrance with the predominant flow out through Chatham Strait, north of Noyes Canyon.

The variation and complexity of the slope morphology increase substantially towards the south from that in Group 4, which is just north of our study area, with more pronounced ridge crests that appear to be associated with rugged, steep relief along the middle and lower slope. The ridgelines are conjugate to the QC Fault Zone and create a series of elongate, margin-parallel topographical boundaries that have step-like discontinuities every 50–100 km. Small canyons and gullies emanating from the shelf edge and down the upper slope appear to converge into higher-order channels that are deflected in a margin-parallel direction along the flanks of the ridges; these channels cross the lower slope and debouche onto the upper rise at discontinuities in the ridges. North of our study area, the QC Fault Zone is located farther seawards (700–2200 m water depths) than in our area and appears to separate the upper slope from the ridgelines that define the morphology of the middle and lower slope. The steepest gradients are located on the seaward-facing flank of the lower slope or along the flanks of margin-parallel ridges in the south.

Geomorphic Group 5 and Group 6 are both located to the west of Haida Gwaii where a very narrow shelf (<10 km) exists and a marine terrace (the ‘Queen Charlotte Terrace’: e.g. Hyndman 2015) dominates the middle and lower slope morphology (Fig. 1) (Brothers *et al.* this volume, in press). These groupings do not include any shelf sea valleys or other major Quaternary sediment delivery pathways from continental mainland (see Brothers *et al.* this volume, in press, their fig. 1b). Bathymetric profiles in Group 5 display a more rounded shelf edge and a series of across-margin bathymetric steps than seen in other profiles. Profiles cross the QC Fault Zone higher on the slope (300–900 m) relative to what is found in Group 4 and Group 6. The margin has an overall convex shape, on average, and profile variation is less than that of Group 4. Group 6 spans the southern half of Haida Gwaii and displays the greatest total relief (3000 m) over the shortest distance (40 km), and the shoreline and shelf edge are nearly coincident (locally as narrow as *c.* 1 km wide) along several stretches of the margin. There are broad margin-parallel valleys that separate the upper slope from ridgelines that define the Queen

Charlotte Terrace and lead to significant along-strike variation. The QC Fault Zone is located in water depths of between 600–2200 m. The largest slides identified in Group 5 and Group 6 appear to be preferentially located along the western flank of the Queen Charlotte Terrace where the gradients exceed 15° (Brothers *et al.* this volume, in press, their fig. 2). Similar to Group 3 and Group 4, the steep, rugged and highly variable bathymetry to the west of Haida Gwaii contains few large slides, but displays widespread evidence for mass-transport activity, particularly along the steep flanks of ridges and along submarine canyon sidewalls.

The maximum extent of glaciation in the Haida Gwaii region occurred from approximately 16 to 15 ka, based on ¹⁴C radiometric age dating (Blaise *et al.* 1990), with deglaciation beginning around 15 ka BP and marine ice-free areas occurring approximately 13.5–13.0 ka (Barrie & Conway 1999). During the LGM, Haida Gwaii appears to have acted as an ice shadow preventing the glaciers from extending westwards onto the narrow western shelf of the archipelago, and thus starving the area of glacially derived sediment. However, during deglaciation, a flood of sediment was introduced to the shelf and slope of western Haida Gwaii from small alpine glaciers, which acted as point sources for sediment supply to the canyons and gullies along the shelf and slope of the archipelago, thus bypassing the shelf and upper slope, and with little blanket sedimentation taking place. Due to the lack of significant sedimentation during the Holocene these erosional features were preserved as seafloor expressions and not buried. This abrupt cessation of sediment supply appears to have occurred around 14.5 ± 0.5 ka with little or no significant Holocene sediment being deposited afterward (Blaise *et al.* 1990; Barrie & Conway 1999).

Methods

Multibeam swath bathymetry was acquired off the west coast of Haida Gwaii between 2009 (cruise ID: 2009002PGC) and 2010 (cruise ID: 2010003PGC), and in the Dixon Entrance area in 2017 (cruise ID: 2017003PGC; Barrie *et al.* 2013, 2018) using a hull-mounted, Kongsberg 0.5° × 1.0° EM710™, dual-swath, multi-sector stabilization, chirp-pulse, high-definition beam-forming system, which operates at a frequency of 70–100 kHz. The surveys were carried out from the Canadian Coast Guard Ship (CCGS) *Vector* at a survey speed of 10 knots in cooperation with the Canadian Hydrographic Service and the Geological Survey of Canada. The tracks were positioned so as to image 100% of the seafloor with 50–100% overlap. Positioning was accomplished with broadcast differential GPS and the multibeam data

were corrected for sound velocity variations in the stratified water column using sound speed casts. The data were edited for spurious bathymetric and navigational points, and subsequently processed using CARIS[®] HIPS and SIPS software. The data were gridded at 5 m resolution, exported as ASCII files, and imported into ArcInfo[®] software for analysis and image production. The beam-forming feature of the EM710 multibeam system reduces the footprint at nadir to around 5 m at 400 m water depth and about 13 m at 1000 m water depth. Thus, by gridding the data at 5 m the data are under-sampled above shallower than 400 m and over-sampled at depths greater than 400 m water depth. In addition, a single MBES line collected in August 2016 along the base of the slope offshore of Haida Gwaii Islands imaged well-defined slumps using a hull-mounted Simrad EM302[™] 30 kHz system aboard the University of Alaska, Fairbank's R/V *Sikuliaq* (Fig. 2a: cruise SKQ2016-11T; <http://www.rvdata.us/>). Cores have not yet been collected along the base of the slope in this area.

The investigation of the southern and central parts of the QC transform fault system was undertaken using the CCGS *John P. Tully* in September 2015 (cruise ID: 2015004PGC) to determine fault geometry and activity. A Knudson[™] low-power, 12-element, 3.5 kHz high-resolution CHIRP (Compressed High Intensity Radar Pulse) seismic-reflection profiling system was used to image the subsurface stratigraphy and to select sampling sites, but little penetration was obtained (on average <5 m). We interpreted the CHIRP seismic-reflection data using both the Knudson[®] Post Survey and the Kingdom Suite[®] software packages. A Simrad EK60[™] 18-kHz single-beam echosounder was used to identify water-column bubble plumes. A large (0.75 m³) IKU grab sampler and a Benthos[™] piston corer were used to collect seafloor sediment, and a GSC 4K underwater drop camera system was used to photograph the seafloor. All sediment cores were analysed using a Geotek[™] Multi-Scan Core Logger (MSCL), which measured density, P-wave velocity and magnetic susceptibility. The cores and grab samples were initially described aboard ship. The cores were split, examined, described and sub-sampled at the land-based sediment laboratory of the Geological Survey of Canada's Pacific Geoscience Center in Sidney, BC. At this laboratory, the split cores were run through the Royal Roads University MSCL-XZ logger to collect high-resolution images, and to measure at high-resolution magnetic susceptibility, bulk density (by gamma-ray attenuation measurements) and P-wave velocities.

Radiocarbon dating was performed at the Keck Carbon Cycle AMS Facility at the University of California, Irvine, California, USA. A local reservoir correction ($\Delta t \pm R$) of 400 years was used, in

addition to the global reservoir correction. These dates are from shell fragments recovered in the cores, which could be older than the dates measured as they may have been transported from upslope or down canyons or gullies and may not record accurate depositional ages. Therefore, we use these ages as a relative estimate of sediment deposition times.

Results

Results from the fieldwork suggest that the QC Fault System is a knife-edge plate boundary between the Pacific and North American plates. In addition, it appears that the fault system is characterized by leakiness, including fluids and gases that are emanating from fractures and faults that comprise the system. The northern segment of the system (referred to here as the northern segment of the QC Fault Zone), extending from the Fairweather Mountain Range in Alaska southwards to where it connects with what we refer to here as the central segment of the QC Fault Zone (located north of Haida Gwaii), has been characterized as a leaky transform fault. This is due to the Edgecumbe volcano offshore of Sitka, Alaska, cited as an example of leakiness associated with magmatic processes (Brew *et al.* 1969; Riehle *et al.* 1992; Greene *et al.* 2007). At the southern segment of the QC Fault Zone two cone-shaped features have been reported to have fluid plumes emanating from their crests (Barrie *et al.* 2013) but the origin of the fluids and the cones is unknown. The recent discovery of a cone emanating fluids from its crest in the central part of the system (central QC segment), offshore of Dixon Entrance, along with newly discovered fluid plumes offshore of NW Haida Gwaii suggest that fluid and gas leakage in the vicinity of the fault zone is fairly common (Fig. 3). We describe the geomorphology of submarine slides in our study area based on landslide classification of Varnes (1978), as well as the submarine slides classification of both Hampton *et al.* (1996) and Greene *et al.* (2002).

Base of central Haida Gwaii slope

The largest and highest concentration of submarine slides located in the central Haida Gwaii slope area are found indented into what appears to be a terrace-like feature, possibly the Queen Charlotte Terrace as described by Hyndman (2015), along the western edge of the terrace, which are well-imaged in the *Sikuliaq* data (Figs 2b & 4). Generally, these submarine slides appear as square-headed block slides, a type of translational slide (after Varnes 1978) and associated block glides ranging in area from approximately 0.56–10.20 km² for distinct single slope failures (see Fig. 4a, b) and upwards to 26.63 km² for compound (multiple merging) slides (Fig. 4c, d).

MASS TRANSPORT ALONG QUEEN CHARLOTTE FAULT ZONE

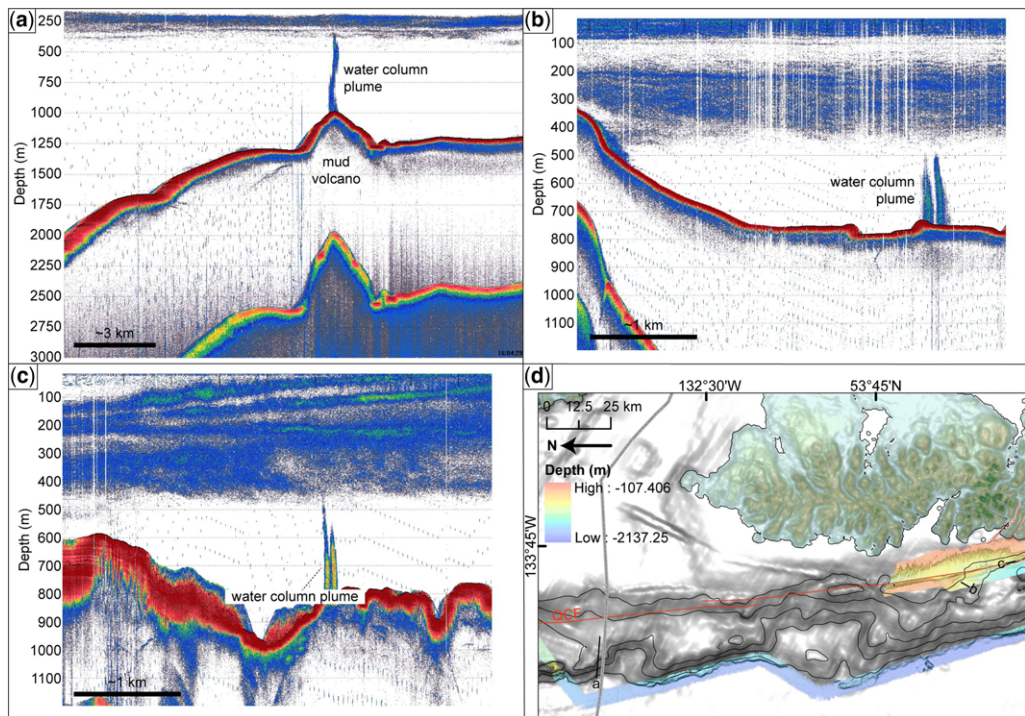


Fig. 3. Examples of 18 kHz profiles and their locations showing sites of gas venting: (a) gas plume of the Dixon Entrance mud volcano; (b) gas plumes at the distal edge of Rift Ridge slide at the base of the glide block; (c) gas plumes at mouths of gullies near the QC Fault Zone north of Cartwright Canyon; and (d) location map showing the position of profiles illustrated in previous (a)–(c) (note the large re-entrant near the location of a, which might be a slide but is not well imaged and thus not discussed).

The headwalls (main or crown scarps) are generally steep (near-vertical) and high (c. 800 m) with the tops of the scarps located at approximately 1000–2000 m water depth. The aggregate of these submarine slides produce distinct scalloped morphology to the base of the slope in this area (Fig. 2b). Most all of the slides appear geomorphically youthful, as the images display sharp well-defined edges and scarps.

Interpretation of the *Sikuliaq* MBES data indicates that the landslides generally increase in size in our study area from north to south (Fig. 2b). These slides also appear to be most concentrated offshore and downslope of where the upper slope is heavily gullied and where two small submarine canyons are located. An obliquely north–south-orientated ridge appears to separate the upper slope from the lower slope (Fig. 2b). The floors of the excavation zones all appear to be at the same depth, on flat surface.

Northern submarine slides. In the northern part of the study area three separate, relatively small, submarine slides notch the flat terrace-like feature at the base of the slope (Fig. 4a). These three slides have head (crown) scarp lengths of 2.30, 0.85 and

0.75 km, respectively, from north to south, and each slide has an irregular, hummocky excavation area of approximately 0.75 km (Fig. 4a). The depositional area extends from 0 to nearly 0.75 km for the northermost larger slide and approximately 0.75 km for the two more southern slides. The estimated area of mass movement in these three slides is approximately 3.45, 1.28 and 1.13 km², respectively. All three submarine slides appear to head at a depth of approximately 2000 m.

Northern compound slide and block glide. Further south, a double-headed compound slide and associated block-glide zone is imaged in detail (Figs 2b & 4b). Here two separate head scarps are seen: the larger with a width of approximately 3 km and the other at approximately 1.5 km. The southern part of the larger slide is less steep than elsewhere and is composed of irregular, hummocky material that has not been completely excavated with a relatively large slumped block sitting at the base of the rubble. The total excavation area is approximately 0.75 km wide and 4.5 km long, covering an area of 3.38 km². A minimum run-out zone that includes

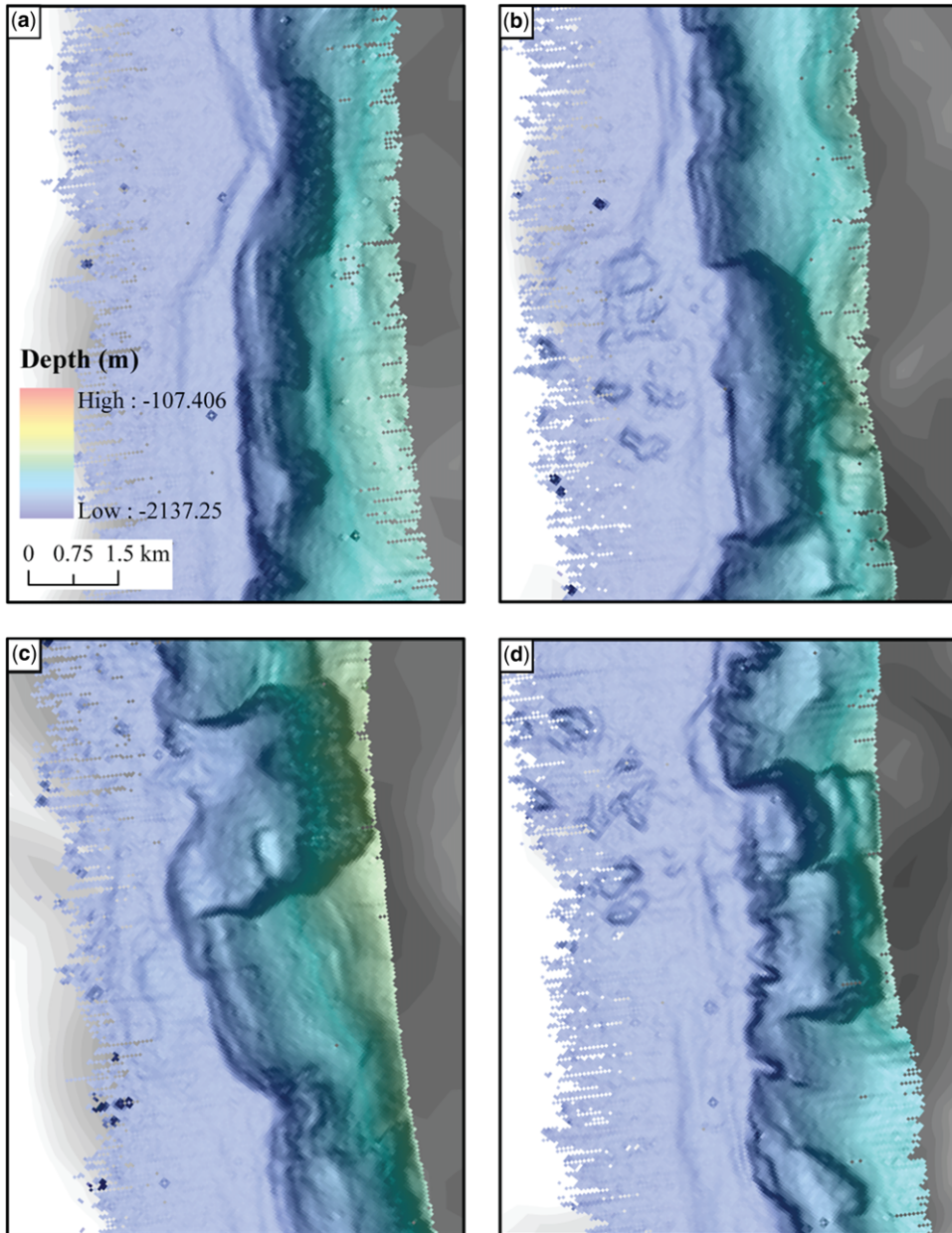


Fig. 4. Expanded views of submarine slides imaged from the *Sikuliaq* multibeam echosounder bathymetry at the base of the central Haida Gwaii slope: (a) the northernmost and smaller slides imaged at the base of the slope; (b) large (c. 26.25 km²) block glides and slides; (c) large (c. 13.5 km²) translational slide and block glide; and (d) large (18.56 km²) compound block glide slide. See Figure 2 for the locations.

many block glides extends outwards from the base of the main scarps for 4.5 km and is about 5 km wide. The total area of the submarine slide is about 26.25 km². A similar but smaller double-headed slump is located just north of this failure.

Central translational block-glide slide. A well-defined translational and block-glide submarine slide is located at the base of the slope just offshore of where extensive gullying occurs on the upper slope (Figs 2b & 4c). The head scarp is not vertical

MASS TRANSPORT ALONG QUEEN CHARLOTTE FAULT ZONE

but composed of irregular, hummocky material that produces a general inclined surface approximately 1 km long and 3 km wide. The excavation zone is approximately 3 km wide, 1.5 km long and includes a large block glide near the base of the upper southern sidewall. Small, scattered glide blocks can be seen extending outwards from the excavation zone for another 1.5 km. The total area of the excavation part of the submarine slide is approximately 10.2 km²; however, the total area including the entire depositional area is not measurable at present because of the narrow data coverage, but could be as large as 13.5 km².

Southern compound block-glide slump. A distinct compound slide consisting of three main scarps is located at the base of the slope in the southern part of our study area (Figs 2b & 4d). The northern slide's main scarp is approximately 1.5 km wide but exhibits its head and crown cracks defining two incipient rotational slump blocks upslope from the steeply dipping main scarp that are of the same width as the crown scarp and extend upslope for at least 0.75 km. Two excavation zones, approximately 1.5 and 0.75 km wide, are associated with this slide and have a floor (sole) several hundred metres deeper than in the companion slumps to the south. The debris lobe, illustrated by many block glides, extends outwards for 3.75 km from the distal edge of the excavation zone and is at least 3.75 km wide.

The southern part of this compound slump is composed of two adjoining main scarps: one approximately 1.5 km wide and the other approximately 1 km wide (Fig. 4d). The main scarps appear less steep than the northern slump, with the excavation zones being approximately the same length, at 0.75 km, but considerably wider, at approximately 2.25 km. Therefore, the total slumped and excavated area is approximately 4.5 km², and, if the debris field imaged in the data (which is c. 3.75 m wide and 3.75 m long, covering a total area of 14.06 km²) is included, then the entire submarine slide appears to cover at least 18.56 km².

Upper central Haida Gwaii slope

The surface expression of the QC Fault Zone is well imaged offshore of the west-central Haida Gwaii (Figs 2b & 5). Here, one of the larger submarine canyons along the western margin of Haida Gwaii heads at the shelf break, and is informally named here 'Cartwright Canyon' (Fig. 5). Gullies at the lower part of the upper slope east of the fault zone are all truncated along the fault zone. Channels south of Cartwright Canyon and the distal upper slope, and larger gullies north of the canyon, all appear to be fluid-induced as they exhibit rilling, retrogressive slumping and slump movement down-gully; similar

to what has been described in the Santa Barbara Channel and in the Monterey Bay region (Eichhubl *et al.* 2001; Greene *et al.* 2002), and described for the gullies in this region (Harris *et al.* 2014). Evidence for present-day fluid flow and/or gas venting was observed in an 18 kHz acoustic water-column profile collected across the mouth of a gully just south of Cartwright Canyon and in close proximity to the QC Fault Zone (Figs 3b, d & 5). Two additional gas plumes were imaged in the 18 kHz dataset during the 2015 *Tully* cruise (Fig. 3b, c). One was emanating from the mouth of a gully truncated by the QC Fault Zone just south of Cartwright Canyon (Figs 3d & 5a) and north of a heavily gullied slope that appears to represent fluid-induced gulling (Figs 3c & 5a), and all were associated with hummocky slopes that are likely to be fluid-induced slumps. The other emanates from the base of a submarine slide glide block at the distal edge of the large Rift Ridge slide located east of the fault zone and north of the rift valley opening (Fig. 5a).

To the north, a rift valley associated with the QC Fault Zone is well-imaged in the MBES data (Fig. 5). An opening in the rift valley is located near the southern part of a high bedrock ridge that tapers downwards toward the south, narrowing and terminating at the mouth of Cartwright Canyon where reverse drainage occurs, blocks sediment transport to the east and directs it southwards (Fig. 5a). Here the image indicates that the rift valley is filling and acts as a sediment conduit. The large (c. 18 km²) submarine slide, which exhibits fluid flow (Fig. 3b) near its toe, appears to have excavated a substantial part of this ridge (Fig. 5b).

A series of core stations (18 in total, numbered in Fig. 5a) were occupied in the area to determine sediment type and ages. Selected core logs are shown in Figures 6 & 7, and dates obtained from the cores are shown in Table 1.

Cartwright Canyon slumps. Small- to medium-sized slumps are imaged in the MBES data both north and south of, and in and adjacent to, Cartwright Canyon (Fig. 5c). Within Cartwright Canyon, retrogressive slumping of canyon deposits appear to be occurring, as well as failures along the upper part of its lower northern wall (Fig. 5c). Immediately to the north of the canyon mouth, a lateral spread submarine slide classified after Varnes (1978), consisting of a scalloped main scarp 1.25 km long with an excavation zone about 0.25 km wide, represents a failure along the lower part of a truncated spur whose submarine slide deposit is buttressed against an uplifted fault scarp located north of the eastern channel of the canyon. The entire slide including the excavation zone and depositional area covers approximately 3.5 km². A smaller arcuate slump (as per Hampton *et al.* 1996) along the southern

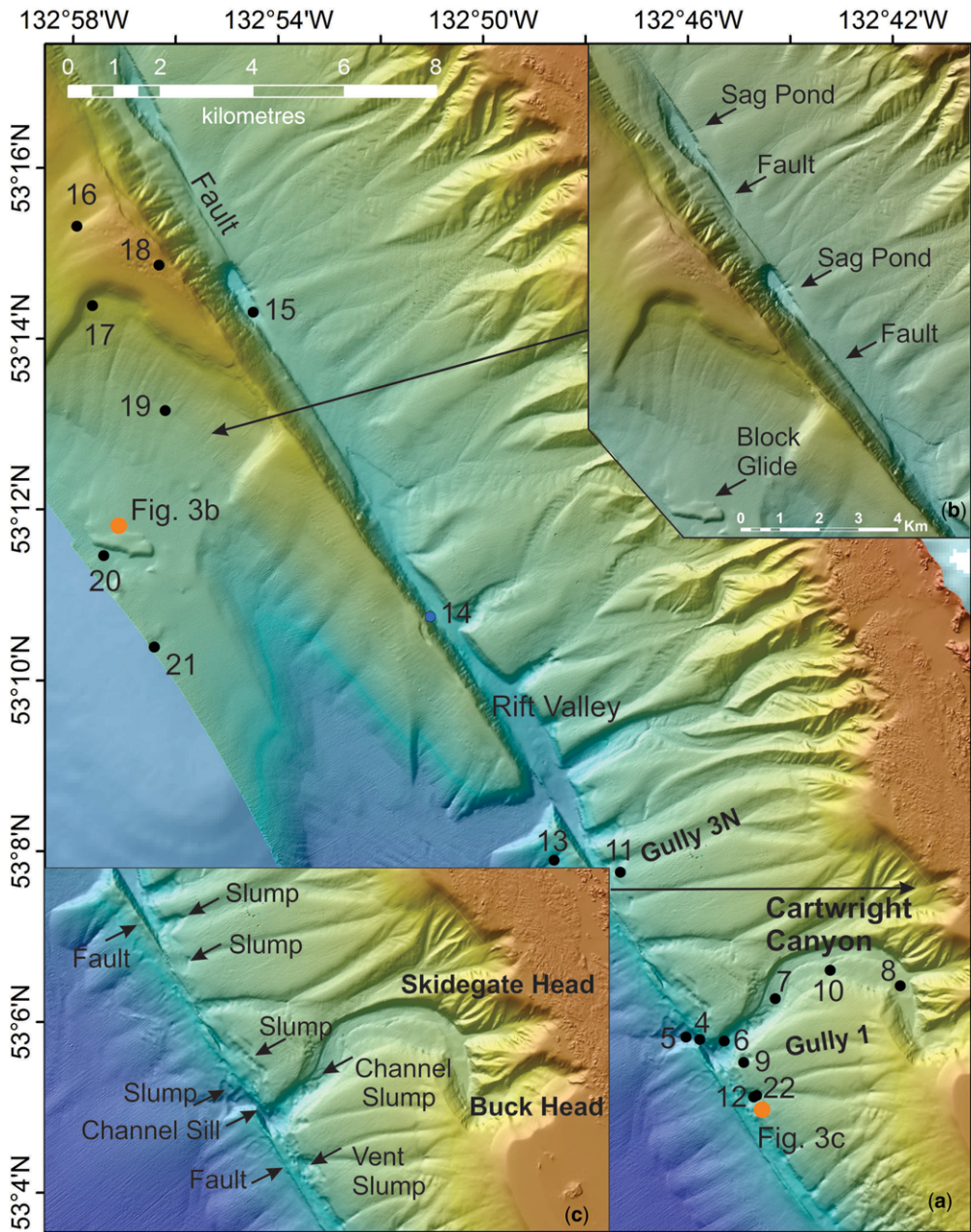


Fig. 5. Upper central Haida Gwaii slope study area: (a) Canadian Hydrographic Service multibeam echosounder bathymetry in the vicinity of Cartwright Canyon and the QC rift valley offshore Haida Gwaii with piston core stations shown as numbered solid black dots and seep locations shown as solid orange dots; (b) expanded view of large (c. 18 km²) translational block glide slide and sag ponds within the QC Fault Zone; and (c) expanded view of the Cartwright Canyon area showing fluid-induced slumps associated with gullies; note the linearity of the fault zone.

part of the slide appears to be evacuating slide debris into the channel of the canyon and a similar type of slide is located on the northern wall of the

lower channel east of the fault zone (Fig. 5c). Small slumps are also observed dipping into the fault zone further north of Cartwright Canyon and south of the

MASS TRANSPORT ALONG QUEEN CHARLOTTE FAULT ZONE

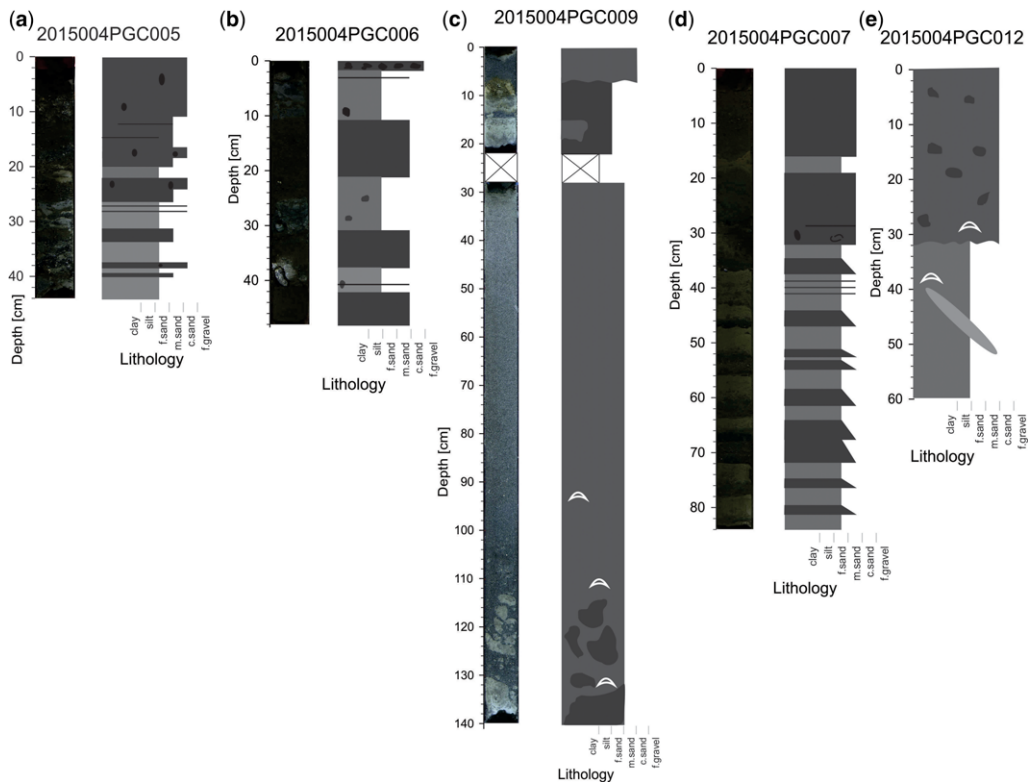


Fig. 6. Core descriptions and logs of the Cartwright Canyon area: (a) Core 2015004PGC005 located in the western offset channel of the canyon; (b) Core 006 located in the non-offset channel of the canyon just east of the QC Fault Zone; (c) Core 009 located at the mouth of 'Gully 1' near the QC Fault Zone; (d) Core 007 located upchannel in the canyon near a retrogressive slump east of the QC Fault Zone; and (e) Core 012 in the mouth of the gully south of canyon (see Fig. 5a for core locations).

rift opening, east of the fault zone at the mouths of gullies including 'Gully 3N', and west of the fault zone as gullied block glides (Fig. 5a).

South of Cartwright Canyon a hummocky slope near the mouth of a gully indicates slope failures (Fig. 5c). At this location a slump on the southern part of the gully exhibits a main scarp 0.75 km long and a disturbed zone of 0.5 km wide covering an area of approximately 0.38 km². Further south the slope east of the fault zone is heavily gullied and exhibits many small slumps (Fig. 5a).

Four core samples recovered near and within Cartwright Canyon close to the QC Fault Zone are described here. At Station 2015004PGC004, no core was recovered but the sediment in the core catcher (<10 cm thick) contained gravel-sized fragments of volcanic rock (basalt) in what appears to be a geomorphic sill in a channel or possible slump block separating the eastern Cartwright Canyon channel from its western extension (Fig. 5a, c). A very short (44 cm) core was recovered at Station

2015004PGC005 (Figs 5a & 6a) in the western offset channel of Cartwright Canyon, at the base of a slump, near the fault and containing interbedded, moderately sorted, gravelly coarse sand and silt beds up to 10 cm in thickness. This material had a density of 2–2.4 g cm⁻³, magnetic susceptibility of generally over 150×10^{-5} SI and a ¹⁴C date of $39\,080 \pm 690$ years BP obtained from a shell fragment taken at 38–40 cm depth in the core. Another short (48 cm) core of hard dense sand and mud was recovered in the thalweg of lower Cartwright Canyon at Station 2015004PGC006 (Figs 5a & 6b), in a flat area closest to, and east of, the fault zone, and below the scarp of a retrogressive slump. This core contained interbedded dark grey clay and dark olive grey fine sand with minor mud balls in clay beds, and a basal unit (38–41 cm deep) of angular mafic pebbles. Density in the core was measured at 2–2.1 g cm⁻³ and magnetic susceptibility at 200×10^{-5} SI. A longer (84 cm) core with eight fining-up sequences in sand overlying

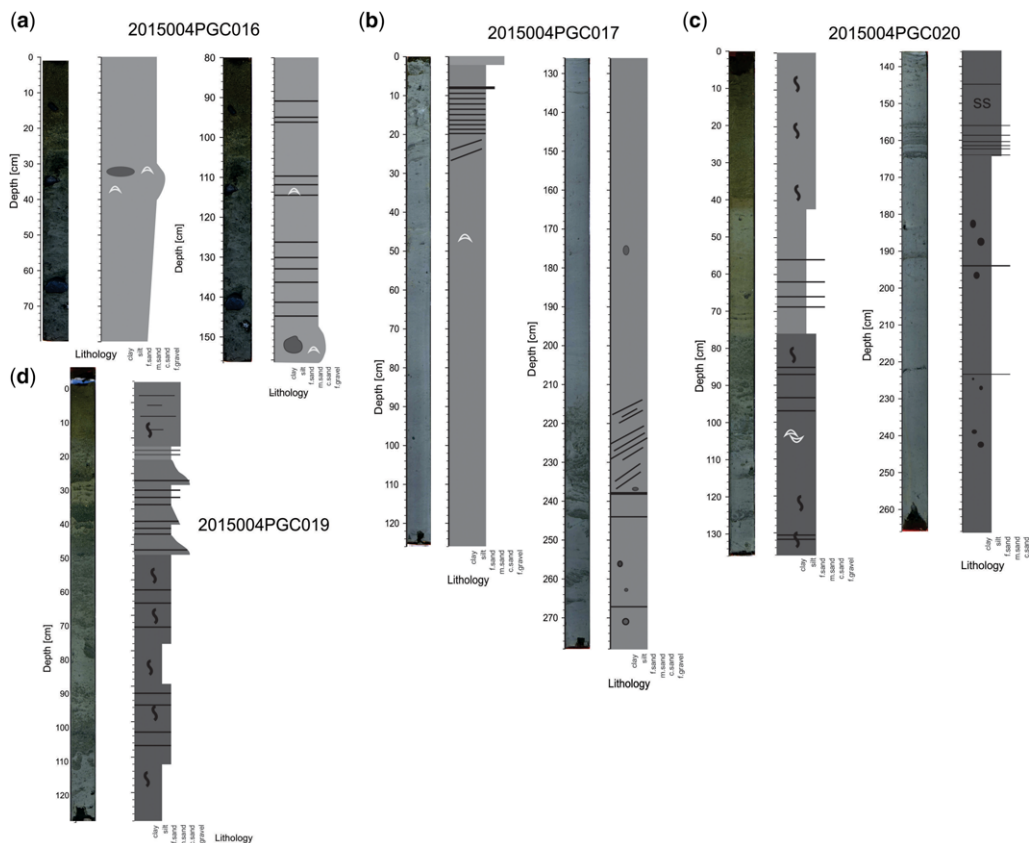


Fig. 7. Core descriptions and logs of the Rift Ridge slide area: (a) Core 2015004PGC016 in undisturbed seafloor on the slope above the head scarp of the slide; (b) Core 017 located at the base of the head scarp of the slide; (c) Core 020 located near the distal edge of the excavation zone near the base of a block glide; and (d) Core 019 located on the floor of the excavation zone (see Fig. 5a for core locations).

mud was recovered at Station 2015004PGC007 located in the middle part of Cartwright Canyon, up-canyon from Core 006, in the lower part of a meander above what appears to be a retrogressive slump within the channel (Figs 5a & 6d). This core recovered interbedded very dark grey fine and very fine sand and mud with minor gravel down to about 30 cm where grading occurs and bedding is repetitive, alternating from olive grey to dark olive grey fine to very fine sand beds interbedded with mud, identified as turbidites from the initial examination of the core. Density was measured at $1.8\text{--}2.2\text{ g cm}^{-3}$ and magnetic susceptibility at between $100\text{ and }275 \times 10^{-5}\text{ SI}$, with the highest values at the top of the core (10–30 cm deep).

A short core (80 cm) was recovered at the confluence of two gullies just south of Cartwright Canyon at Station 2015004PGC012 (Figs 5a & 6e). Lithology in this core consists of olive grey poorly sorted gravelly sand with minor shell and

mud, and possible distorted laminations with a sand lens extending from 40 to 55 cm deep. Density of the core was measured at $2\text{--}2.3\text{ g cm}^{-3}$ and magnetic susceptibility varied from approximately $25 \times 10^{-5}\text{--}225 \times 10^{-5}\text{ SI}$, with the highest values at the upper part (10–30 cm deep) of the core. Another core (Station 2015004PGC022) attempted just up the gully from Station 2015004PGC012 had no recovery, with a just small amount of sand found in the core catcher (Fig. 5a).

Cores recovered from the mouths of prominent gullies (informally named ‘Gully 1’ and ‘Gully 3N’: Fig. 5a) both south and north of Cartwright Canyon and near the QC Fault Zone are described here. A short (140 cm) core (Core 2015004PGC009) recovered at the upper reaches of a gully (informally called ‘Gully 1’: Fig. 5a) located just south of Cartwright Canyon has a stratigraphy composed of very dark grey mud to fine sand over olive grey sandy silt with sand clasts down to 22 cm. From 28 to

MASS TRANSPORT ALONG QUEEN CHARLOTTE FAULT ZONE

Table 1. Radiocarbon dates obtained from piston cores collected during the 2015 CCGS John P. Tully cruise

Laboratory No. UCIAMS	Sample No.	Cruise No.	Station No.	Core depth (cm)	Material	¹⁴ C age ± years BP
167532	201504-0539	2015004PGC	5	38–40	Shell	39 080 ± 690
167533	201504-09129	2015004PGC	9	129	Shell	42 870 ± 1100
167534	201504-1528	2015004PGC	15	27–29	Shell	21 320 ± 80
167535	201504-1631	2015004PGC	16	31	Shell	13 450 ± 35
167536	201504-1648	2015004PGC	16	48	Shell	49 390 ± 2500
167537	201504-16165	2015004PGC	16	165	Shell	16 190 ± 45
167538	201504-1928	2015004PGC	19	27–28	Shell	14 110 ± 40
167539	201504-1940	2015004PGC	19	39–41	Shell	13 620 ± 35
167540	201504-20109	2015004PGC	20	109	Shell	20 980 ± 80

Dates obtained primarily from pelecypod shell fragments buried in the sediment (transported).

113 cm the core contains dark olive grey massive fine–medium sand with minor shell fragments; and from 113 to 140 cm sand and silt rip-up clasts were found (Fig. 6c). Measured density in the core ranged from 2.1 to 2.3 g cm⁻³, magnetic susceptibility measured from just below 200 × 10⁻⁵ SI at the top of the core gradually increased to nearly 350 × 10⁻⁵ SI at 125 cm deep, and a ¹⁴C date from a shell fragment of 42 870 ± 1100 years BP at 129 cm was obtained. Two other core stations were occupied north of Cartwright Canyon including Station 011 near a submarine slide head scarp within the mouth of a major gully ('Gully 3N': Fig. 5a) but this had poor core recovery with only stiff mud obtained in the core catcher. Similarly, nothing was recovered from Station 013 in the first gully south of the rift opening on the west side of the fault zone.

Rift Ridge submarine slide. The Rift Ridge slide is a large translational block-glide slide (after Varnes 1978) that has an approximate 6 km-long, 100 m-high main scarp and a 3 km-wide gullied excavation zone, covering an area of approximately 18 km², with the crown and top of the main scarp located in approximately 400 m of water (Barrie *et al.* 2013) (Fig. 5b). A large block glide is located 1.5 km downslope from the distal edge of the excavation zone in what appears to be a fairly extensive debris field, although the total area of the field is indeterminate due to incomplete MBES coverage. The main scarp and sidewalls at the head of the slump are rounded and less sharp in outline than the deeper slides imaged at the base of the slope.

Six piston core stations (2015004PGC016–2015004PGC021) were occupied within and adjacent to the Rift Ridge slide (Fig. 5a), and all recovered cores with little penetration into the seafloor. Cores taken at stations 2015004PGC016 and 2015004PGC018 were from undisturbed seafloor above the head of the slump, with just a core-catcher recovery at Station 2015004PGC018 and little

recovery from Core 016. The other core stations are within the landslide, with Core 2015004PGC021 recovering a sample from the core catcher only.

At Station 2015004PGC016, a 170 cm-long core was recovered consisting of olive grey medium–coarse sand with pebbles and mud (poorly sorted) throughout, and with foraminifer down to 31 cm where a shell fragment was taken for dating. From 31 to 35 cm a large cobble was found, and from 35 to 170 cm olive grey mud with shell and sand laminations and some gravel and cobbles was recorded, becoming muddier with depth; a large (2.5 cm) pebble (siliciclastic) and shell fragments were located at the base (Fig. 7a). The density of the core was measured at 2.0–2.4 g cm⁻³, and magnetic susceptibility was measured at between 250 × 10⁻⁵ and 500 × 10⁻⁵ SI. Ages within the core were obtained by ¹⁴C radiocarbon dates from shell fragments dated at 13 450 ± 35 years BP at 31 cm, 49 390 ± 2500 years BP at 40–48 cm and 16 190 ± 45 years BP at 165 cm (Figs 5 & 7a; Table 1).

Core 2015004PGC017 was obtained at the foot of the NE edge of the main scarp of the Rift Ridge slide and recovered a 277 cm-long core that contained 20 cm of olive grey fine sand with shell fragments unconformably (erosional boundary at 20 cm) overlying massive grey mud with minor intervals of laminations, ice-rafted debris (IRD) and rare shell fragments. From 216 to 234 cm, disturbed laminations with minor IRD are present (Fig. 7b). Density of the core measured 1.9–2.4 g cm⁻³, and magnetic susceptibility ranged between 200 × 10⁻⁵ and 300 × 10⁻⁵ SI, except just above the erosional boundary (20 cm deep) and at the disturbed zone (216–234 cm deep) where magnetic susceptibility approached and exceeded 400 × 10⁻⁵ SI.

At Station 2015004PGC018, located in undisturbed seafloor at the crest of the rift ridge, and just east of the Rift Ridge slide head scarp (Fig. 5a), only a core catcher jammed with mud was recovered. At Station 2015004PGC019, located on the floor of

the excavation zone, 128 cm of core was recovered (Figs 5a & 7d). The stratigraphy consisted of a thin (*c.* 20 cm-thick) weakly bedded olive grey fine sand that overlies a 10 cm-thick olive-coloured mud layer that in turn overlies dark olive grey interbedded fine-medium sand and mud about 22 cm thick (Fig. 7d). Density in the core was measured at 1.0–2.3 g cm⁻³, and magnetic susceptibility alternated between 200×10^{-5} and 400×10^{-5} SI. We obtained two ¹⁴C dates of $14\,110 \pm 40$ years BP from a shell fragment at 27–28 cm and another of $13\,620 \pm 35$ years BP from another shell fragment at 39–41 cm.

At Station 2015004PGC020, located at the distal edge of the slide near the foot of the glide block, a 257 cm core of mud was recovered. The stratigraphy of the core consisted of olive grey massive bioturbated sandy mud down to about 40 cm, overlying olive grey massive to laminated silty clay that extends down to about 73 cm deep and overlies very dark grey bioturbated to laminated sandy mud extending down to about 155 cm deep, which overlies dark grey clay with minor gravel and laminations (Fig. 7c). Density in the core was measured at 1.7–2.2 g cm⁻³, with magnetic susceptibility ranging from 75×10^{-5} to nearly 400×10^{-5} SI, with the lowest measurement found in the massive to laminated silty clay (*c.* 60–70 cm deep) and the highest in the bioturbated laminated sandy mud (from 80 to 190 cm). A ¹⁴C date of $20\,980 \pm 80$ years BP from a shell fragment at 109 cm was obtained (see Table 1).

Dixon Entrance (mud volcano). A mud volcano venting gas was discovered on the slope west of Dixon Entrance during the 2015 cruise of the *Tully*. Recently (August 2017), the CCG vessel *Vector* collected MBES data over the volcano (Barrie *et al.* 2018) (Fig. 8), which shows that the volcano sits on a north–south-orientated ridge, exhibits submarine slides along the western and southern base of the ridge, and has a south-trending circular-headed valley bordering the eastern margin of the volcano. Two medium-sized submarine slides are well-imaged in the recently collected Canadian Hydrographic Service MBES bathymetry data, including a rotational slump measuring 3.1 km along a subtle approximately 130 m-high main scarp whose crest lies 1060 m deep, and has a head and secondary block with possible vent sites. The main body of the slide lies at a depth of 1190 m and extends a minimum of 0.69 km out from the head block, with the entire imaged part of the slide covering an area of 2.14 km². The other medium-sized slide is located at the base of the southern end of the ridge upon which the mud volcano sits and appears to be a debris avalanche (see Varnes 1978), not fully imaged, with a main scarp that measures 3.7 km long and a head slump block at the base

of the southern part of the main (crown) scarp. This slide has an excavation zone of at least 2 km, with the slide covering an area of at least 7.40 km². Smaller slides notch the western base of the north–south-orientated ridge, which extends approximately 3 km north from the crater of the mud volcano (Fig. 8). Along the SE flank of the ridge, a flat-floored valley measures 2.70 km wide and 4.40 km long, sloping down from a depth of 1170–1290 m and extending for a minimum of 2.6 km. An apparent incipient slump, that is not fully imaged and is evidenced by a subtle arcuate crown or head scarp that is a minimum of 8.8 km long, lies at a depth of 1172 m with a base at 1230 m that is undercut by the gullied head of a large landslide (previously described). This incipient slide has a potential excavation zone of >4.4 km, covering an area of at least 38.7 km² and defined by irregular arcuate ridges or ripples (possible compression ridges) and troughs characteristic of creep and a weakly gullied slope (Fig. 8).

To the south of the mud volcano, three core stations (2015004PGC028–2015004PGC030) were occupied in the vicinity of the QC Fault Zone (Fig. 9a). Core 2015004PGC028 was obtained near a slump west and downslope of the QC Fault Zone where a 106 cm-long core consisting of an upper olive grey, muddy to fine sand layer with foraminifera, 30 cm thick, overlies a 12 cm-thick olive grey mud with muddy sand and laminations (Fig. 9b). Beneath these upper layers, but within the upper 42 cm of the core, are olive grey mottled muddy sand and mud that gradually grade downwards into olive mud with sand and subtle colour laminations and foraminifera near the bottom of the core at approximately 85 cm deep. Density measurements ranged from 1.6 to 1.95 g cm⁻³, being greatest in the upper laminated zone (30–34 cm deep), and magnetic susceptibility varying between 75×10^{-5} and nearly 225×10^{-5} SI in the upper 45 cm of the core, and generally being less than 100×10^{-5} SI below 45 cm (Fig. 9b).

Core station 2015004PGC029 was located in a gully on the Dixon Entrance slope and recovered 38 cm of olive-coloured massive, medium-sorted, fine-medium sand that overlies olive-coloured sandy gravel (gravel size up to 4 cm in diameter) at 30 cm deep (Fig. 9c). Density was measured at 2–2.4 g cm⁻³ within the core and magnetic susceptibility averaged about 100×10^{-5} SI, except at the gravel layer (30 cm deep) where it approached nearly 300×10^{-5} SI.

Core station 2015004PGC030 was located in a sediment pond west of the fault where 66 cm of cored sediment was recovered. The sedimentary stratigraphy consists of interbedded dark olive grey sandy mud and dark grey gravelly clay with an erosional base at 40 cm deep, and overlies very

MASS TRANSPORT ALONG QUEEN CHARLOTTE FAULT ZONE

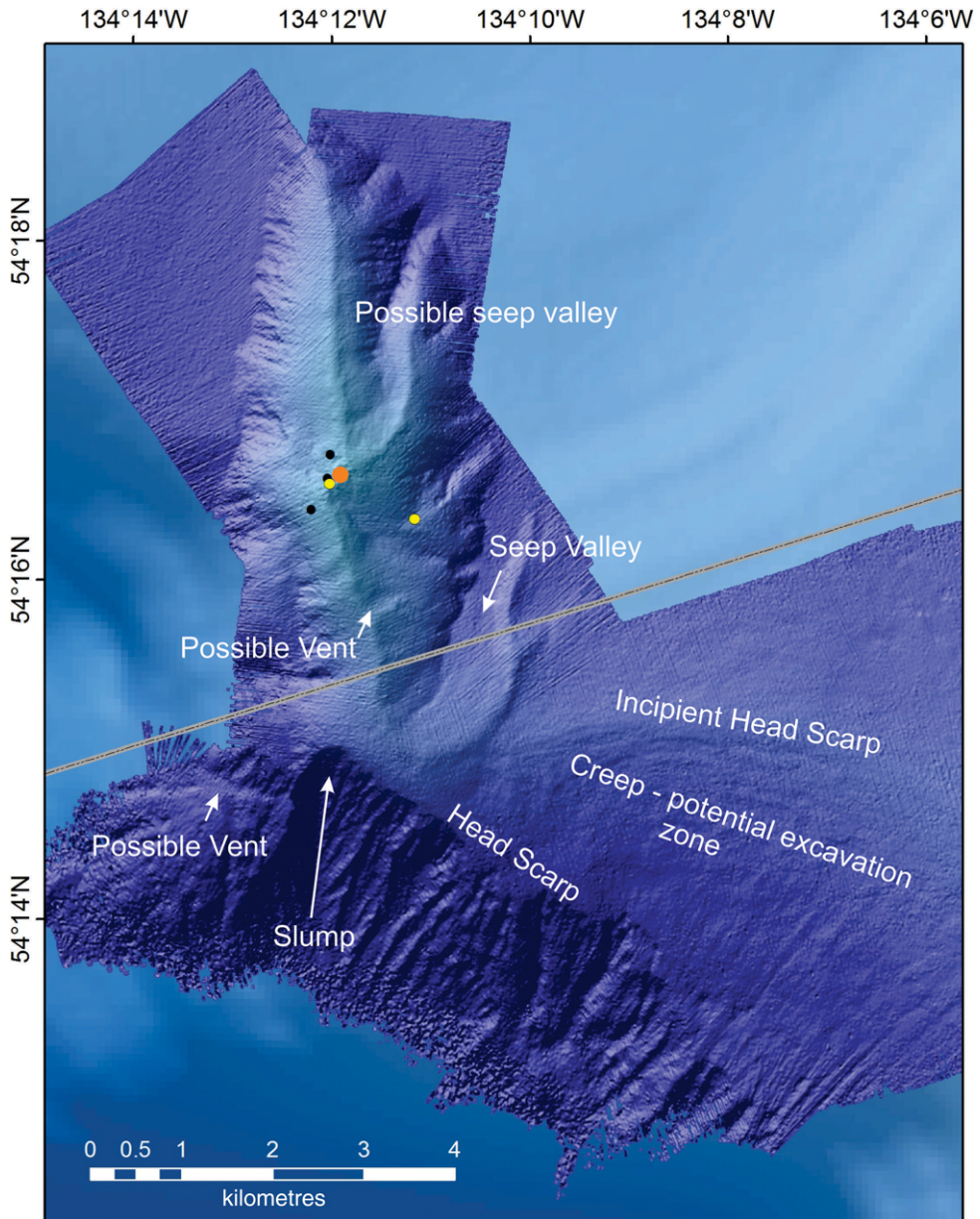


Fig. 8. The Dixon Entrance study site with the 2017 *Vector* MBES bathymetric image of the recently (2015) discovered mud volcano showing two medium-sized ($c. 2.14\text{--}7.40 \text{ km}^2$) submarine slides at the base of the western and southern flanks of a north-south-orientated ridge upon which the volcano sits and a circular-headed fluid-induced-like valley at the base of the eastern flank; locations of three IKU grab samples are shown as black dots; the main vent is shown as a large solid orange dot; and camera drop locations are shown as small yellow dots, with drop 2015004PGC031 at the crest of the ridge near the vent (orange dot) and 037 further down the flank about half-way between the vent and the seep valley.

dark laminated clay, which in turn overlies graded coarse-fine sand and laminated silt (Fig. 9d). Density was measured at $1.8\text{--}2.2 \text{ g cm}^{-3}$ and magnetic

susceptibility ranged from about 120×10^{-5} to approximately 225×10^{-5} SI, with the highest reading (225×10^{-5} SI) occurring within the laminated

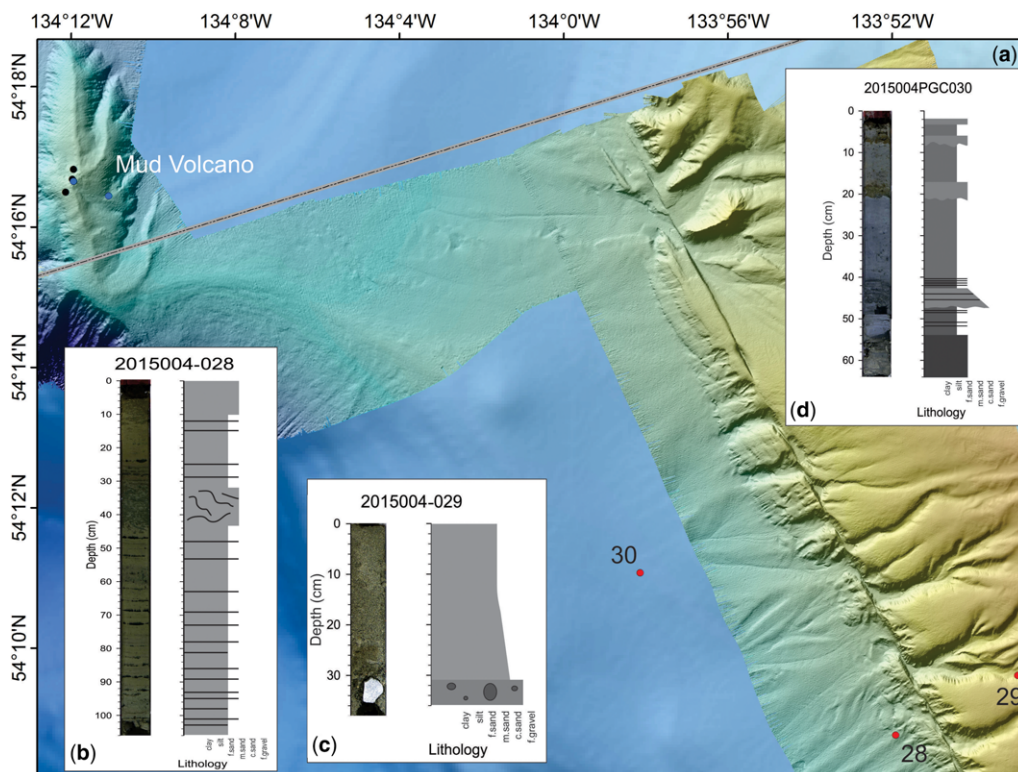


Fig. 9. Recently (2017) collected MBES bathymetry of the Dixon Entrance area: (a) showing the mud volcano with the locations of three IKU samples (small black dots) and the locations of piston cores (numbered small red dots); (b) Core 2015004PGC028 located west and downslope of the QC Fault Zone; (c) Core 029 located in a gully east of the QC Fault Zone; and (d) Core 030 located far down the slope east of the QC Fault Zone. Seep sites shown as blue dots.

clay unit at 45 cm deep. No datable material was recovered from these cores.

In addition to the cores described above, two drop camera short-tow transects (stations 2015004PG C031 and 2015004PGC037; Figs 8 & 9a) were made to photograph the seafloor in the vicinity of the mud volcano during the 2015 *Tully* cruise. Five IKU grab sampler sites were selected from the photographs. Excellent photographs were obtained during the camera drops, which indicated that methane gas was emanating from the cone of the mud volcano. Evidence of methane is given by the presence of methanogenic chemosynthetic communities consisting of tentatively identified *Calyptragenia* spp. clams (Fig. 10), a *Vestimentiferan* spp., tubeworm, *Beggiatoa* spp. bacterial mats and carbonate slabs. No lava or outcrops of volcanic rock were photographed. In contrast, gravel, pebbles and cobbles covering a mud slope were observed, with many of the clasts being rounded. However, angular fragments of dark-coloured rock were seen in the photographs. Small narrow rivulets of mud

were also observed. The five IKU grab samples (2015004PGC032–2015004PGC036, photographs P180, P88, P309, P238 and P90, respectively) were full of mud/clay, gravel, clams, mussels and carbonate-cemented mud slabs.

A 3.5 kHz CHIRP seismic-reflection profile collected across the mud volcano (along the same transect as the 18 kHz profile showing the gas plume: Fig. 3a, d) illustrates the hard seafloor of the mud volcano that is most likely to be the result of carbonate cementation associated with the gas vent and seeps (Fig. 11). The profile is characteristic of most of the 3.5 kHz sub-bottom data collected and illustrates that the seafloor along the QC Fault Zone in our study area is dense.

Discussion

The MBES images of the QC Fault Zone collected by the Canadian Hydrographic Service illustrate the linearity of the structure offshore of western

MASS TRANSPORT ALONG QUEEN CHARLOTTE FAULT ZONE

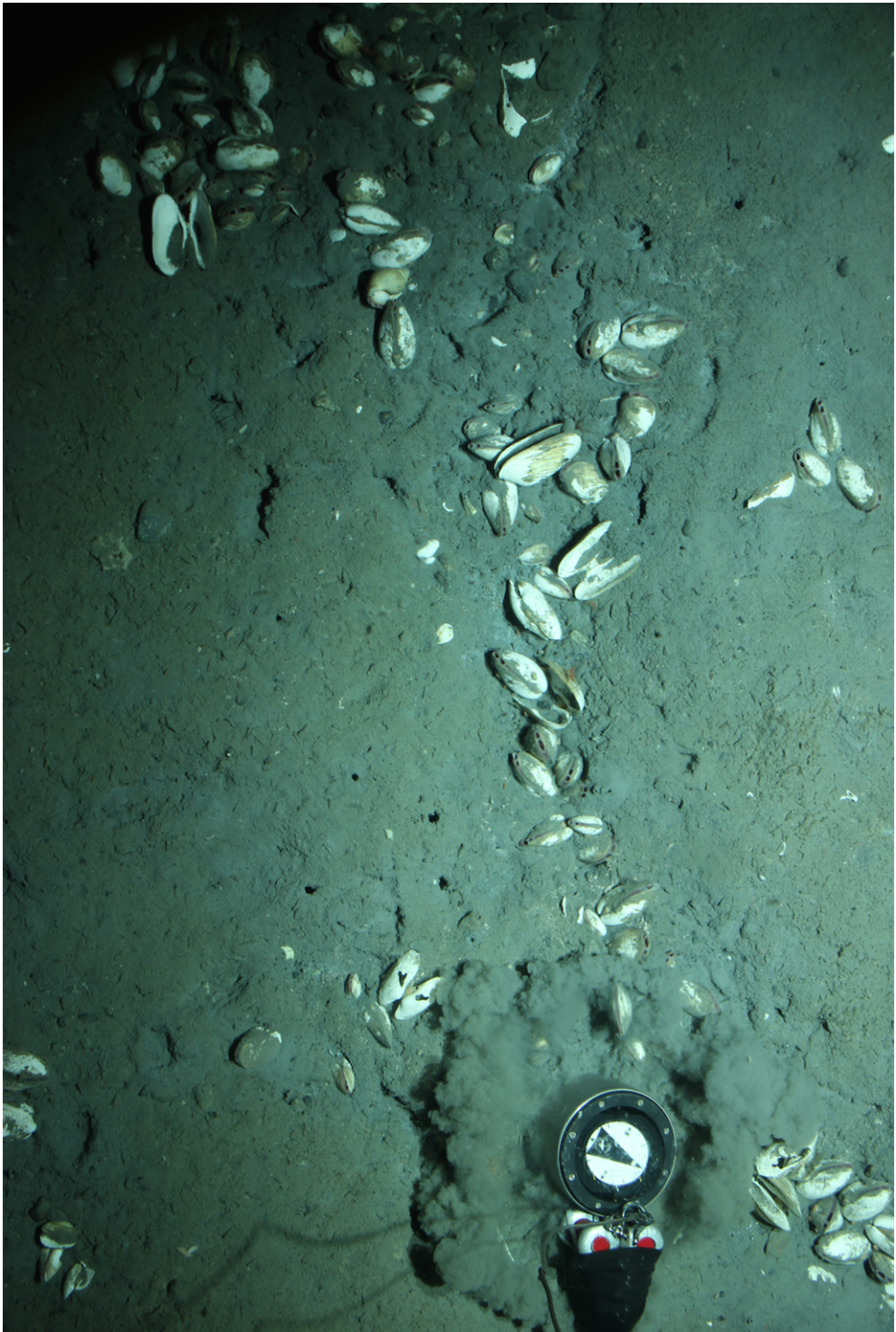


Fig. 10. Seafloor photograph near the main vent site of the mud volcano off Dixon Entrance, Alaska showing chemosynthetic clams (*Caliptogena* spp.), which appear to be associated with the methane seep.

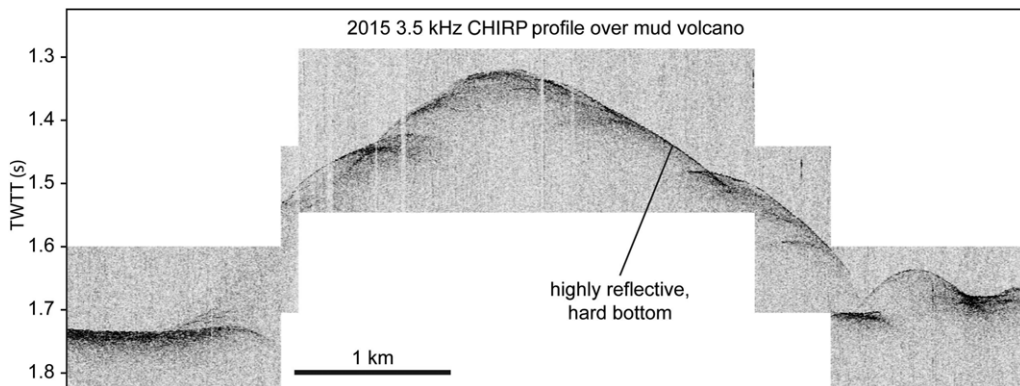


Fig. 11. A 3.5 kHz profile across the newly discovered (2015) mud volcano on the Dixon Entrance slope showing a hard-density seafloor, probably the result of carbonate cementation precipitated from gas venting from the volcano. This profile is characteristic of most 3.5 kHz profiles collected in the study areas, which indicate a high-density substrate. TWT, two-way travel time.

Haida Gwaii and that many small submarine slides are present on the upper slope which appear to be fluid-induced (see Fig 5). With the exception of one large submarine slide on the upper slope (Rift Ridge slide: Fig. 5), the larger submarine slides are located at the base of the slope, as shown in the *Sikuliaq* bathymetric data (see Figs 2 & 4). We speculate that the differences in the character and sizes of these submarine slides result from differing sedimentary processes, and the tectonic and glacial history of the region.

Tectonics

The QC–FW Fault Zone is a major plate boundary that separates the Pacific Plate from the North American Plate and, as such, is seismically active, resulting in many large magnitude earthquakes through geological time that could have stimulated mass failures along the western Haida Gwaii slope. However, with the exception of the likely fluid-induced submarine slides on the upper slope, no evidence has been found that indicates major large mass failures on the slope east of the QC Fault Zone west of Haida Gwaii. Sediment recovered in our coring campaign consists largely of dense sands and muds (50% $>2.0 \text{ g cm}^{-3}$, 90% $>1.8 \text{ g cm}^{-3}$) that may have been compacted by seismic shaking throughout the late Pleistocene and Holocene (age dates from cores range from ^{14}C $49\,390 \pm 2500$ to $13\,450 \pm 35$ years BP, which refer to the maximum age of the sediments: see Table 1); while in contrast the blocky nature of the large slumps at the base of the slope suggests that the failed materials there are probably less dense and more muddy than on the upper slope.

Core subsamples selected for ^{14}C radiometric dating show three major ages for the sediment

recovered along the western margin of Haida Gwaii, consisting of 44 ka calibrated, 25 ka calibrated and 14 ka calibrated ^{14}C years BP (Table 1). This suggests that little sediment younger than 14 (^{14}C) = 17 ka (calibrated) exist in the areas cored because of significant sedimentation shutdown after the retreat of the glaciers, which is consistent with dates obtained by Blaise *et al.* (1990) and Barrie & Conway (1999).

Fluid flow

The apparent mud volcano on the continental slope just west of Dixon Entrance discovered during the *Tully* cruise of 2015 is a well-defined cone-like structure with a crest located at 1000 m water depth. At the time of the survey, the cone was profusely venting gas 700 m into the water column from within a small crater at the crest, as shown in the 18 kHz sounder profile (Fig. 3a). The newly discovered mud volcano indicates that gas is venting along the slope in this region, and we surmise that the slope is locally unstable because of the presence of gas and other fluids in the sediment. Two medium-sized submarine slides, a circular-headed flat-floored valley and many small sediment failures at the base of a north–south-orientated ridge that the volcano sits upon indicate that mass wasting is occurring (see Fig. 8). This geographical situation allowed for the concentration of late Pleistocene glacial material, and Holocene terrestrial and pelagic organic-rich sediments which were deposited on the slope to eventually produce gas (methane) that accumulated and migrated through the sediment, increasing pore pressures that eventually led to instability and mass failures. Continuous deposition appears to have provided sediment in quantities that could accumulate

MASS TRANSPORT ALONG QUEEN CHARLOTTE FAULT ZONE

without being compacted by seismicity, resulting in mass failures.

We did not sample the gas, but speculate that it contains methane as chemosynthetic (methanogenic) communities in the form of high concentrations of apparent living *Calyptogena* clams and mussels that were observed in the bottom photographs and sampled with the IKU grab (Fig. 10). In addition, extensive areas of carbonate slabs and chimneys, apparent *Biggiotoa* bacterial mats, and a single *Vesimentiferin* tubeworm were observed in the bottom photographs close to the vents, which also suggest the presence of methane.

The 3.5 kHz sub-bottom profiles (e.g. Fig. 11) obtained during the 2015 geophysical investigation and recently collected by CCGS *Vector* MBES data offshore Dixon Entrance show the existence of other cone-like features (possible vents in Fig. 8) and a hummocky and deformed seafloor characteristic of slides (Fig. 5). We noted that Core 2015004PGC030, which is one of the cores recovered furthest away from the QC Fault Zone (see Fig. 9), had one of the lowest undisturbed, non-turbidite densities measured ($1.8\text{--}2.2\text{ g cm}^{-3}$) in the area of Dixon Entrance. In contrast, densities of the cores elsewhere in the vicinity of the QC Fault Zone were generally greater, at about $2.0\text{--}2.3\text{ g cm}^{-3}$. Therefore, we infer that the upper continental slope west of Dixon Entrance is unstable and prone to mass wasting, probably the result of fluid flow and gas expulsion.

It appears that gas expulsion and fluid flow are prominent along most of the central QC Fault Zone offshore central Haida Gwaii. We consider this segment of the fault zone to be very leaky, in respect to gas and fluids, along most of its length, as in each of our survey areas we found gas plumes that originate close to, or within, the fault zone and speculate that the faults are acting as conduits for the venting of the gases and fluids. In addition, the gas could be accumulating in antiformal structures that form many of the conjugate ridges of the QC Fault Zone. The gas could have originated from multiple sources such as from the compaction and degradation of organic-rich sediment, as well as from continuously forming hydrocarbon resources (Tinivella & Giustiniani 2013), and dissolution of clathrates or frozen gas hydrate systems (Dimitrov 2000; Depreiter *et al.* 2005; Sauter, *et al.* 2006; Tinivella & Giustiniani 2013). Heat at depth, such as from a magmatic source, also has the potential of producing mud volcanoes (Tinivella & Giustiniani 2013); although this is most common along convergent margins, it also has the potential to occur along transform margins, as indicated by the Edgecumbe volcano along the northern segment of the QC Fault Zone (Brew *et al.* 1969).

The translational and block-glide Rift Ridge slide is the largest located on the upper Haida Gwaii slope,

covering an area of approximately 18 km^2 . This feature is located on what appears to be a transpressional ridge associated with the QC Fault Zone, and we speculate that it may have failed due to seismicity along the QC Fault Zone and possible uplift and steepening of the slope associated with transpression.

Densification of sediment

Our inability to obtain long piston cores within the upper slope areas of the QC Fault Zone because of the high-density and well-packed sediments was surprising. We speculate that the reason for this densification is associated with one of two causes or, perhaps, both. First, during the LGM Haida Gwaii acted as an ice shadow along the continental shelf of British Columbia, preventing the glaciers and glacial-fed sediment from reaching the distal edge of the shelf and upper slope (Barrie & Conway 1999). This created a sediment-starved area west of Haida Gwaii, as indicated by the old ages (late Pleistocene) obtained from ^{14}C dating of shell fragments (see Table 1). Second, the high recurrence level of medium- to large-magnitude earthquakes along the QC Fault Zone may have increased the density of the sediment through shaking and packing (see Fig. 1). Sawyer & DeVore (2015) reported that even though earthquakes are a major stimulant for submarine slides, the most active areas on Earth are surprisingly devoid of such features. These authors' comparative studies of the Deep Sea Drilling Programs' drill cores from active and passive tectonic margins supports the concept of 'seismic strengthening' or densification (consolidation) by *in situ* dewatering put forth by several investigators (McAdoo *et al.* 2000; Locat & Lee 2002; Strozzyk *et al.* 2010; Nelson *et al.* 2011), as active margins have higher undrained shear strength than passive margins. The combination of both a sediment-starved slope and densification could result in a more stable slope that is difficult to penetrate using gravity or piston corers. However, exceptions should occur where fluid flow is present, as gas-charged sediments have lower than normal shear strength (Hampton *et al.* 1996).

The characteristics of the base-of-slope slides (base of central Haida Gwaii slope) contrast with those submarine slides we observe on the upper slope. Most all of the submarine slides on the upper slope appear to be composed of primarily disaggregated materials that result from debris flows and retrogressive slumping stimulated by increased pore pressures associated with fluid flow; at the base of the slope, the slides have a blockier character suggesting intact block glides and translational submarine slides possibly triggered by earthquakes. This difference in character may result from differing sediment regimes, with the upper slope being

influenced by the Haida Gwaii glacial shadow and sediment-starved margin; while the base of the slope received more fine-grained sediment, including pelagic deposition during the Pleistocene and Holocene, and was far enough removed from the seismic activity along the QC Fault Zone not to be subjected to densification.

However, the depositional regime and the presence of fluids in the Dixon Entrance area indicate a less dense environment. A piston core collected from the Dixon Entrance slope (Core 2015004 PGC028) recovered mud that exhibited the lowest densities ($1.6\text{--}1.95\text{ g cm}^{-3}$) of all the cores recovered on the 2015 *Tully* cruise, suggesting that densification of the sediment in this region is not as high as on the central Haida Gwaii slope, within the glacial sediment shadow. Even though the core was located near the QC Fault Zone, fluids within the sediment may play a role in reducing densification here. In addition, Core 201400PGC030 had a lower density ($1.8\text{--}2.2\text{ g cm}^{-3}$) than reported for cores taken on the upper slope west of central Haida Gwaii. Glacial deposition was probably more intense and continuous in the Dixon Entrance region because of the opening from mainland British Columbia to the abyssal plain, although recent studies indicate that glaciers moved primarily to the north rather than west in this region during the LGM (Lyles *et al.* 2017).

Conclusions

Recently collected MBES bathymetric data, 3.5 kHz seismic-reflection profiles, piston cores and camera-tow photographs were used to investigate slope failures and mass-transport processes along western British Columbia, Canada. Three physiographical regions were studied, consisting of: (1) the upper central Haida Gwaii continental slope; (2) the basal central Haida Gwaii continental slope; and (3) the mid-continental slope off Dixon Entrance. Each of the physiographical regions exhibits different types of submarine mass failures that we conclude are related to Quaternary sediment supply, fluid flow and tectonic processes such as seismic activity and transpression. The characteristics that we conclude are diagnostic of the types of mass failures which have occurred along the central QC Fault Zone are as follows.

Upper central Haida Gwaii slope

- High density sand and mud (densities range from 1.6 to 2.4 g cm^{-3}), with the highest densities in areas of no fluid flow, sediment appears to have been compacted by seismic shaking (e.g. Sawyer & DeVore 2015) throughout the late Pleistocene and Holocene, thus increasing slope stability.

- A few small (*c.* $0.4\text{--}1\text{ km}^2$) to medium (*c.* $2\text{--}4\text{ km}^2$) fluid-induced debris flows and retrogressive slumps, locally stimulated by increased pore pressures (e.g. Hampton *et al.* 1996) associated with gas and fluid flow occur within the vicinity of the QC Fault Zone.
- Cores recovered sediment dated no younger than ^{14}C $13\,450 \pm 35$ years BP.
- The sediment glacial shadow margin of Haida Gwaii prevented sediment supply to the area during the last glacial advance.
- An exception to the sizes of failures in this area is the large (*c.* 18 km^2) Rift Ridge slide that may have been stimulated by large magnitude earthquakes, and transpressional uplift and tilting of the slope.

Base of central Haida Gwaii slope

- Mass failures at the base of the central Haida Gwaii slope exhibit different geomorphic characteristics than those failures found on the upper slope.
- The submarine slides appear relatively unweathered and therefore youthful, suggesting recent failures, are more blocky in appearance, and are larger in size (ranging from *c.* 0.56 to 10.20 km^2 for distinct single slope failures and upwards to 26.63 km^2 for compound slides) than observed on the upper slope (see Fig. 2).
- No piston cores have been collected yet in this region, but we suspect that the sediments here are less dense than on the upper slope due to the greater distance the region lies from the QC Fault Zone; thus, earthquakes have less effect on compaction of the slope here than on slopes closer to the fault zone.
- More recent and continuous sedimentation has probably occurred in this area than in areas closer to Haida Gwaii.
- The soles of the slides appear to be on a flat surface along the western edge of the Queen Charlotte Terrace of Hyndman (2015).
- We attribute the lack of densification to the distance the region lies from the QC Fault Zone; thus earthquakes have less effect on the lower slope here than on the upper slope closer to the fault zone.

Dixon Entrance (mud volcano)

- The newly discovered active mud volcano on the mid-continental slope off of Dixon Entrance indicates that considerable gas is venting in the region.
- Camera drop photographs show extensive chemosynthetic communities to be associated with seeps on the volcano (e.g. *Calypptogena*-like clams and mussels, suggesting that the gas contains methane).

MASS TRANSPORT ALONG QUEEN CHARLOTTE FAULT ZONE

- Large areas of carbonate cementation and bacterial mats were found that produce hard (high-density) substrate (see Fig. 11).
- The lowest density (1.6–1.95 g cm⁻³) sediment measured in the cores were found off Dixon Entrance.
- The MBES bathymetric data show that two medium-sized (c. 2.14–7.40 km²) submarine slides indent the western and southern base of a north–south-orientated ridge that supports the volcano.
- Mass failures along the flanks of the mud volcano suggest that pore pressures are high here and that gas-charged sediments may have lower-than-normal shear strengths; thus facilitating failure that may have been, and still can be, stimulated by earthquakes.
- We conclude that the mid-slope region off Dixon Entrance is prone to mass-wasting events due to the close proximity of the seismically active QC Fault Zone, based on the relatively low density of sediments in the region and local gas-charged sediments.

Acknowledgements We wish to thank the Captain and crew of the CCGS *John P. Tully* for their support and encouragement while at sea collecting data. The Canadian Hydrographic Service compiled the bathymetry data. NOAA, NSF and the University of Alaska graciously shared bathymetric data they collected with the R/V *Sikuliaq*. We thank the Royal Roads University for the use of their Geotek split-core multi-sensor core logger. Charlie Endris and Norman Maher assisted in the preparation of the figures. Any use of trade, firm, or product names is for descriptive purposes only and does not imply endorsement by the US Government.

Funding Partial support for this investigation came from the USGS National Earthquake Hazards Reduction Program (NEHRP) to H.G. Greene through a grant to the Sitka Sound Science Center in Sitka, Alaska.

References

- ATWATER, T. 1970. Implications of plate tectonics for the Cenozoic tectonic evolution of western North America. *Geological Society of America Bulletin*, **81**, 3513–3536.
- BARRIE, J.V. & CONWAY, K.W. 1999. Late Quaternary glaciation and postglacial stratigraphy of the northern Pacific margin of Canada. *Quaternary Research*, **51**, 113–123.
- BARRIE, J.V., CONWAY, K.W. & HARRIS, P.T. 2013. The Queen Charlotte Fault, British Columbia: seafloor anatomy of a transform fault and its influence on sediment processes. *Geo-Marine Letters*, **33**, 311–318.
- BARRIE, J.V., GREENE, H.G. *ET AL.* 2018. *The Queen Charlotte–Fairweather Fault Zone—A Submarine Transform Fault, Offshore British Columbia and Southeastern Alaska*. Cruise Report of 2017003PGC CCGS Vector and 2017004PGC CCGS John P. Tully, Geological Survey of Canada, Open File, **3398**, 159.
- BLAISE, B., CLAGUE, J.J. & MATHEWES, R.W. 1990. Time of maximum Late Wisconsin glaciation, west coast of Canada. *Quaternary Research*, **34**, 282–295.
- BOSTWICK, T.K. 1984. *A re-examination of the 1949 Queen Charlotte earthquake*. Msc dissertation, University of British Columbia, Vancouver, Canada.
- BREW, D.A., MULLER, L.J.P. & LONEY, R.A. 1969. Reconnaissance geology of the Mount Edgcombe Volcanic Field, Kruzof Island, southeastern Alaska. In: *Geological Survey Research 1969*. United States Geological Survey, Professional Papers, **650D**, D1–D18.
- BROTHERS, D.S., HAEUSSLER, P. *ET AL.* 2017. A closer look at an undersea source of Alaskan earthquakes, *Eos*, **98**, <https://doi.org/10.1029/2017EO079019>. Published on 15 August 2017.
- BROTHERS, D.S., ANDREWS, B.D. *ET AL.* In press. Slope failure and mass transport processes along the Queen Charlotte Fault: southeastern Alaska. In: LINTERN, D.G., MOSHER, D.C. *ET AL.* (eds) *Subaqueous Mass Movements*. Geological Society, London, Special Publications, **477**, <https://doi.org/10.1144/SP477.30>
- BUFE, C.G. 2005. Stress distribution along the Fairweather–Queen Charlotte transform fault system. *Bulletin of the Seismological Society of America*, **95**, 2001–2008.
- CARLSON, P.R., PLAFKER, G. & BRUNS, T.R. 1985. *Map and Selected Seismic Profiles of the Seaward Extension of the Fairweather Fault, Eastern Gulf of Alaska*. United States Geological Survey, Miscellaneous Field Studies Map, **MF-1722**.
- CENTER FOR COASTAL AND OCEAN MAPPING JOINT HYDROGRAPHIC CENTER. 2010. *Gulf of Alaska—Bathymetry: Law of the Sea Data*, <http://ccom.unh.edu/theme/law-sea/law-of-the-sea-data/gulf-of-alaska> [last accessed September 2017].
- DEPREITER, D., POORT, J., VAN RENSBERGEN, P. & HENRIET, J.P. 2005. Geophysical evidence of gas hydrates in shallow submarine mud volcanoes on the Moroccan margin. *Journal of Geophysical Research*, **110**, B10103, <https://doi.org/10.1029/2005JB003622>, 2005
- DIMITROV, L.I. 2000. Mud volcanoes – the most important pathway for degassing deeply buried sediments. *Earth-Science Reviews*, **59**, 49–76.
- DING, K., FREYMUELLER, J.T., WANG, Q. & ZOU, R. 2015. Coseismic and early postseismic deformation of the 5 January 2013 *M_w* 7.5 Craig earthquake from static and kinematic GPS solutions. *Bulletin of the Seismological Society of America*, **105**, 1153–1164.
- EICHHUBL, P., GREENE, H.G., NAEHR, T. & MAHER, N. 2001. Structural control of fluid flow: Offshore fluid seepage in the Santa Barbara Basin, California. *Journal of Geochemical Exploration*, **69–70**, 545–549.
- GREENE, H.G., MAHER, N. & PAULL, C. 2002. Physiography of the Monterey Bay region and Implications about continental margin development. *Marine Geology*, **181**, 55–82.
- GREENE, H.G., O’CONNELL, V.M., WAKEFIELD, W.W. & BRYLINSKY, C.K. 2007. The offshore Edgcombe lava field, southeast Alaska: geologic and habitat characterization of a commercial fishing ground. In: TODD, B.J. &

- GREENE, H.G. (eds) *Mapping the Seafloor for Habitat Characterization*. Geological Association of Canada, Special Papers, **47**, 277–295.
- HAMPTON, M., LEE, H.J. & LOCAT, J. 1996. Submarine landslides. *Reviews of Geophysics*, **34**, 33–59, <https://doi.org/10.1029/95RG03287>
- HARRIS, P.T., BARRIE, J.V., CONWAY, K.W. & GREENE, H.G. 2014. Hanging canyons of Haida Gwaii, British Columbia, Canada; Fault-control on submarine canyon geomorphology along active continental margins. *Deep-Sea Research Part II: Topical Studies in Oceanography*, **104**, 83–92.
- HYNDMAN, R.D. 2015. Tectonics and structure of the Queen Charlotte Fault Zone, Haida Gwaii, and large earthquakes. *Bulletin of the Seismological Society of America*, **105**, 1058–1075, <https://doi.org/10.1785/0120140181>
- HYNDMAN, R.D. & ELLIS, R.M.. 1981. Queen Charlotte fault zone: microearthquakes from a temporary array of land stations and ocean bottom seismographs. *Canadian Journal of Earth Sciences*, **18**, 776–788.
- HYNDMAN, R.D. & HAMILTON, T.S. 1993. Queen Charlotte area Cenozoic tectonics and volcanism and their association with relative plate motions along the northeastern Pacific margin. *Journal of Geophysical Research*, **98**, 14 257–14 277.
- LAY, T., YE, L., KANAMORI, H., YAMAZAKI, Y., CHEUNG, K.F., KWONG, K. & KOPER, K.D. 2013. The October 28, 2012 M_w 7.8 Haida Gwaii underthrusting earthquake and tsunami: Slip partitioning along the Queen Charlotte Fault transpressional plate boundary. *Earth and Planetary Science Letters*, **375**, 57–7.
- LISOWSKI, M., SAVAGE, J.C. & BURFORD, R.O. 1987. Strain accumulation across the Fairweather and Totschunda faults, Alaska. *Journal of Geophysical Research: Solid Earth*, **92**, 11 552–11 560.
- LOCAT, J. & LEE, H.J. 2002. Submarine landslides: advances and challenges. *Canadian Geotechnical Journal*, **39**, 193–212, <https://doi.org/10.1139/t01-089>
- LYLES, A.S., BAICHTAL, J.F. & KARL, S.M. 2017. Deciphering flow path of ice across the southern Alaska panhandle based on geomorphological interpretation and field data. Poster presented at the Geological Society of America Annual Meeting, 22–25 October 2017, Seattle, Washington, USA.
- MCADOO, B.G., PRATSON, L.F. & ORANGE, D.L. 2000. Submarine landslide geomorphology, US continental slope. *Marine Geology*, **169**, 103–136, [https://doi.org/10.1016/S0025-3227\(00\)00050-5](https://doi.org/10.1016/S0025-3227(00)00050-5)
- NATIONAL GEOPHYSICAL DATA CENTER. 2013. ETOPO1 Global Relief Model. *National Centers for Environmental Information*, <http://www.ngdc.noaa.gov/mgg/global/global.html> [last accessed September 2017].
- NELSON, C.H., ESCUTIA, C., DAMUTH, J.E. & TWICHELL, D.C., JR 2011. Interplay of mass-transport and turbidite system deposits in different tectonic and passive margin continental margin: External and local controlling factors. In: SHIPP, R.C., WEIMER, P. & POSAMENTIER, H.W. (eds) *Mass-Transport Deposits in Deepwater Settings*. SEPM Special Publications, **961**, 9–66.
- PAGE, R.A. 1969. Late Cenozoic movement on the Fairweather fault in southeastern Alaska. *Geological Society of America Bulletin*, **80**, 1873–1878.
- PLAFKER, G., HUDSON, T., BRUNS, T.R. & RUBIN, M. 1978. Late Quaternary offsets along the Fairweather fault and crustal plate interactions in southern Alaska. *Canadian Journal of Earth Sciences*, **15**, 805–816.
- PRIMS, J., FURLONG, K.P., ROHR, K.M.M. & GOVERS, R. 1997. Lithospheric structure along the Queen Charlotte margin in western Canada: constraints from flexural modeling. *Geo-Marine Letters*, **17**, 94–99.
- RIEHLE, J.R., CHAMPION, D.E., BREW, D.A. & LANPHERE, M.A. 1992. Pyroclastic deposits of the Mount Edgecumbe volcanic field, southeast Alaska: eruptions of a stratified magma chamber. *Journal of Volcanology and Geothermal Research*, **53**, 117–143.
- ROGERS, G.C. 1983. *Seismotectonics of British Columbia*. PhD thesis, Department of Geophysics and Astronomy, University of British Columbia.
- ROHR, K.M.M., SCHEIDHAUER, M. & TREHU, A.M. 2000. Transpression between two warm mafic plates: the Queen Charlotte Fault revisited. *Journal of Geophysical Research*, **105**, 8147–8172.
- SAWYER, D.E. & DEVORE, J.R. 2015. Elevated shear strength of sediments on active margins: evidence for seismic strengthening. *Geophysical Research Letters*, **42**, 10 216–10 221, <https://doi.org/10.1002/2015GL066603>
- SAUTER, E.J., MUYASKSHIN, S.I. ET AL. 2006. Methane discharge from a deep-sea submarine volcano into the upper water column by gas hydrate-coated methane bubbles. *Earth and Planetary Science Letters*, **243**, 354–365.
- STROZYK, F., STRASSER, M., FORSTER, A., KOPF, A. & HUHN, K. 2010. Slope failure repetition in active margin environments: Constraints from submarine landslides in the Hellenic fore arc, eastern Mediterranean. *Journal of Geophysical Research*, **115**, B08103, <https://doi.org/10.1029/2009JB006841>
- TINIVELLA, U. & GIUSTINIANI, M. 2013. An overview of mud volcanoes associated to gas hydrate system. In: NEMETH, K. (ed.) *Updates in Volcanology – New Advances in Understanding Volcanic Systems*. Intech, Rijeka, Croatia, 225–267, <https://doi.org/10.5772/51270>
- TREHU, A.M., SCHEIDHAUER, M., ROHR, K.M.M., TIKOFF, B., WALTON, M.A.L., GULICK, S.P.S. & ROLAND, E. 2015. An abrupt transition in the mechanical response of the upper crust to transpression across the Queen Charlotte Fault. *Bulletin of the Seismological Society of America*, **105**, 1114–1128.
- VARNES, D.J. 1978. Slope movement types and processes. In: SCHUSTER, R.L. & KRIZEK, R.J. (eds) *Transportation Research Board, Special Report 176: Landslides – Analyses and Control*. National Research Council, Washington, DC, 11–33.